# Supplementary Materials

Zhipeng Wang[1], Davit A Potoyan[1], and Peter G Wolynes[1]

[1] *Center for Theoretical Biological Physics, Department of Chemistry and Department of Physics and Astronomy, Rice University, Houston TX 77005*

## 1 The Histogram Estimator for the Distribution of DNA sites' Unbinding Rates

We assume the decoy sites' binding free energies ($\Delta G_b$) take a normal distribution, which indicates that $\ln k_{doff} \sim \mathcal{N}(\Delta\hat{G}, \sigma^2)$. We adopt a 15-bin equally-spaced histogram to approximate the distribution of $\ln k_{doff}$ by dividing the distribution into 15 non-overlapping intervals, where each bin represents a decoy site with the corresponding unbinding rate. The historgram estimator enables us to use 15 different decoy species with different unbinding rates to approximate the distribution of unbinding rates of the whole population of decoy sites. Monte Carlo Simulations can be readily performed by treating the whole population of decoy sites as 15 different reacting chemical species, each with the different unbinding kinetic rate determined by the histogram estimator.

The histogram estimator developed by the statistics community[2] also considers further about determining the optimal band width of histogram bins to acheive better goodness-of-fit, as well as the bias-variance tradeoff of statistical estimations. Those are beyond our current focus and need. In this paper we adopted the simple division of the distribution of unbinding rates into 15 bins with the equal band width. We choose 15 bins as it is accurate enough to approximate the distribution while keeping the total number of chemical species in the reacting system relatively small to facilitate reasonably fast Monte Carlo Simulations. If the number of bins increases, the approximation will be more unbiased, but the total number of chemical species in Monte Carlo Simulations will grow thus it will slow down the simulation. Here we choose the appropriate bin numbers to balance out the problem of "curse of dimensionality" and the accuracy of approximations.

## 2 Chemical Reactions and Kinetic Parameters

The chemical reactions and the corresponding kinetic parameters are listed in Table 1.

Table 1: Chemical Reactions for $I\kappa B\alpha/NF\kappa B$ regulatory circuit. The parameters of the feedback cycle originate from the work of Hoffmann et al [1] while the ranges of values for specific binding/unbinding rates come from binding microarray data [4] and in vitro kinetic measurements [3, 5].

| Reactions | Rate coeff | Values |
|---|---|---|
| $D_U + N_n \rightarrow D_B$ | $k_{don}$ | $10\mu M^{-1}min^{-1}$ |
| $D_B \rightarrow D_U + N_n$ | $k_{doff}$ | $\sim LogNormal(\Delta\hat{G}, \sigma^2)$ |
| $OFF + N_n \rightarrow ON$ | $k_{on}$ | $10\mu M^{-1}min^{-1}$ |
| $ON \rightarrow OFF + N_n$ | $k_{off}$ | $1min^{-1}$ |
| $D_B + I_n \Rightarrow D_U + NI_n$ | $k_s$ | $[0-10]\,\mu M^{-1}min^{-1}$ |
| $ON + I_n \Rightarrow OFF + NI_n$ | $k_s$ | $[0-10]\,\mu M^{-1}min^{-1}$ |
| $ON \Rightarrow ON + mRNA$ | $k_{tr}$ | $1.03\mu Mmin^{-1}$ |
| $mRNA \Rightarrow mRNA + I_c$ | $k_{tl}$ | $0.2448min^{-1}$ |
| $mRNA \Rightarrow \emptyset$ | $k_d$ | $0.017min^{-1}$ |
| $I_c \rightarrow I_n$ | $k_{in}$ | $0.018min^{-1}$ |
| $I_n \rightarrow I_c$ | $k_{out}$ | $0.012min^{-1}$ |
| $N_c \rightarrow N_n$ | $k_{Nin}$ | $5.4min^{-1}$ |
| $N_c + I_c \rightarrow NI_c$ | $k_f$ | $30\mu M^{-1}min^{-1}$ |
| $NI_c \rightarrow N_c + I_c$ | $k_b$ | $0.03min^{-1}$ |
| $N_n + I_n \rightarrow NI_n$ | $k_{fn}$ | $30\mu M^{-1}min^{-1}$ |
| $NI_n \rightarrow N_n + I_n$ | $k_{bn}$ | $0.03min^{-1}$ |
| $NI_c \Rightarrow N_c$ | $\alpha$ | $[0.10-0.55]\,min^{-1}$ |
| $NI_n \Rightarrow NI_c$ | $k_{NIout}$ | $0.83min^{-1}$ |

# 3 Abbreviation and Full names in Chemical Reactions

Table 2: Names of species and their numbers

| Abbreviation | Full name |
|---|---|
| $D_B$ | Bound Decoy Site |
| $D_U$ | Unbound Decoy Site |
| $ON$ | Active gene state |
| $OFF$ | Inactive gene state |
| $I_n$ | Nuclear $I\kappa B\alpha$ |
| $I_c$ | Cytoplasmic $I\kappa B\alpha$ |
| $N_n$ | Nuclear $NF$–$\kappa B$ |
| $N_c$ | Cytoplasmic $NF$–$\kappa B$ |
| $NI_n$ | Nuclear $NF$–$\kappa B - I\kappa B\alpha$ complex |
| $NI_c$ | Cytoplasmic $NF$–$\kappa B - I\kappa B\alpha$ complex |
| $N \equiv N_n + N_c + NI_n + NI_n + D_B$ | Total number of $NF$–$\kappa B$: $10^5$ |
| $Gene \equiv ON + OFF$ | Total number of $Genes$: 1 |
| $D \equiv D_B + D_U$ | Total number of natural $Decoys$: $2 \times 10^4$ |

# 4 Comparison of SPR-determined unbinding rate $k_{off}$ and and PBM-determined z scores for p65-p50 heterodimers

In order to convert the z-scores determined by Protein Binding Microarray (PBM) [4] to unbinding rates of DNA binding sequences for p65-p50 heterodimers, we use the data in [4] of unbinding rates ($k_{off}$) for mice p65-p50 heterodimers determined by Surface Plasmon Resonance (SPR) (six independent SPR measurements). We did the linear regression of $\ln(\ln 2/k_{off})$ over the corresponding z-scores, which is the same as the authors did for c-Rel-c-Rel and p50-p50 homodimers. The linear regression curves and the corresponding R squares and linear regression equation are shown in Figure 1:

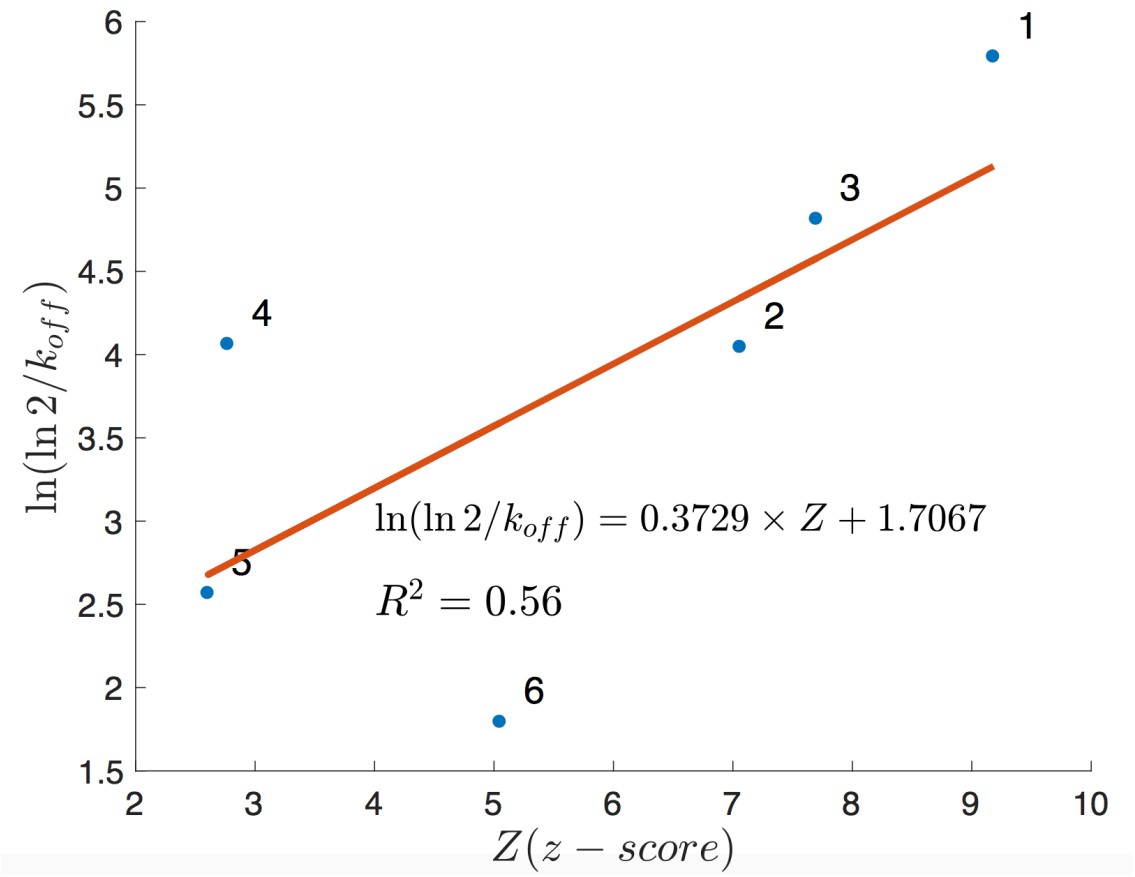


Figure 1

Figure 2: Linear regression of SPR-determined unbinding rate $k_{off}$ over the PBM-determined z scores for mice p65-p50 heterodimers. Data is determined from six independent measurements (SPR data).

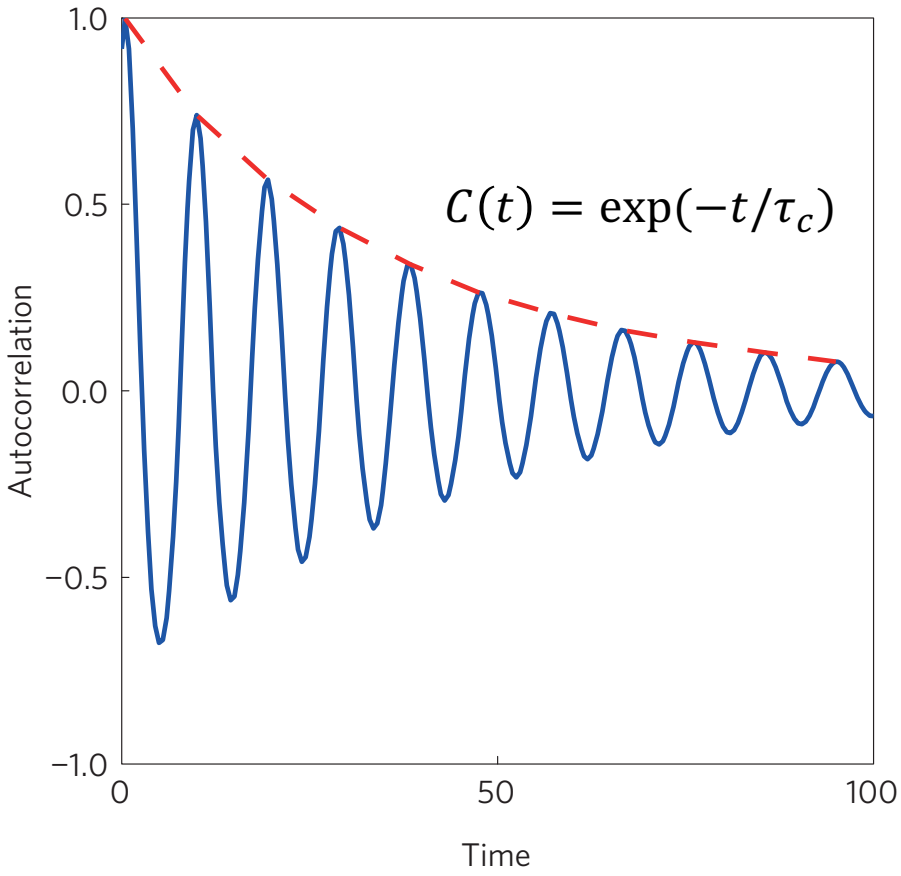


Figure 3: **The instruction of quantifying temporal coherence of stochastic oscillatory dynamics.** In Figure 3, the examplary Periodic Normalized Autocorrelation function is illustrated (plotted in a blue line), and the red dash line represents an exponential decay fitted to the envelope of that autocorrelation function. The oscillation quality thus can be further calculated by $\tau_c/T$ in which $T$ is the oscillation period.

# 5 Supplemental Figures

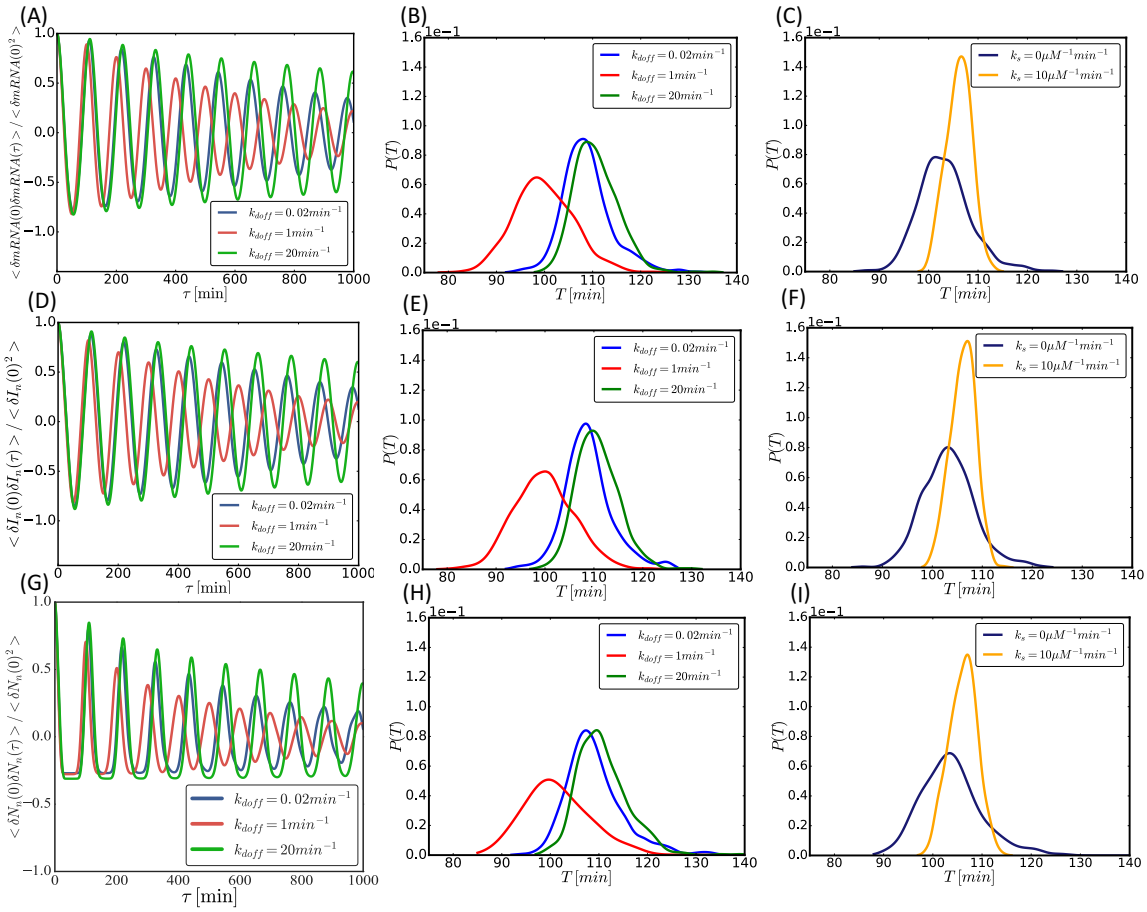


Figure 4: (A) Normalized Autocorrelations of steady-state fluctuations of $mRNA$ population for identical DNA sites with different unbinding rates ($\alpha = 0.25min^{-1}$). (B) Distribution of Oscillation Period (T) of $mRNA$ population for different unbinding rates ($\alpha = 0.25min^{-1}$).(C) Distribution of oscillatory period (T) of $mRNA$ population for the case of distributed binding sites and distributed sites with molecular stripping enabled ($\alpha = 0.25min^{-1}$). (D) Normalized Autocorrelations of steady-state fluctuations of nuclear $I\kappa B(I_n)$ population for identical DNA sites with different unbinding rates ($\alpha = 0.25min^{-1}$). (E) Distribution of Oscillation Period (T) of $I_n$ population for different unbinding rates ($\alpha = 0.25min^{-1}$).(F) Distribution of oscillatory period (T) of $I_n$ population for the case of distributed binding sites and distributed sites with molecular stripping enabled ($\alpha = 0.25min^{-1}$).(G) Normalized Autocorrelations of steady-state fluctuations of nuclear free $NF\kappa B(N_n)$ population for identical DNA sites with different unbinding rates ($\alpha = 0.25min^{-1}$). (H) Distribution of Oscillation Period (T) of $N_n$ population for different unbinding rates ($\alpha = 0.25min^{-1}$).(I) Distribution of oscillatory period (T) of $N_n$ population for the case of distributed binding sites and distributed sites with molecular stripping enabled ($\alpha = 0.25min^{-1}$).

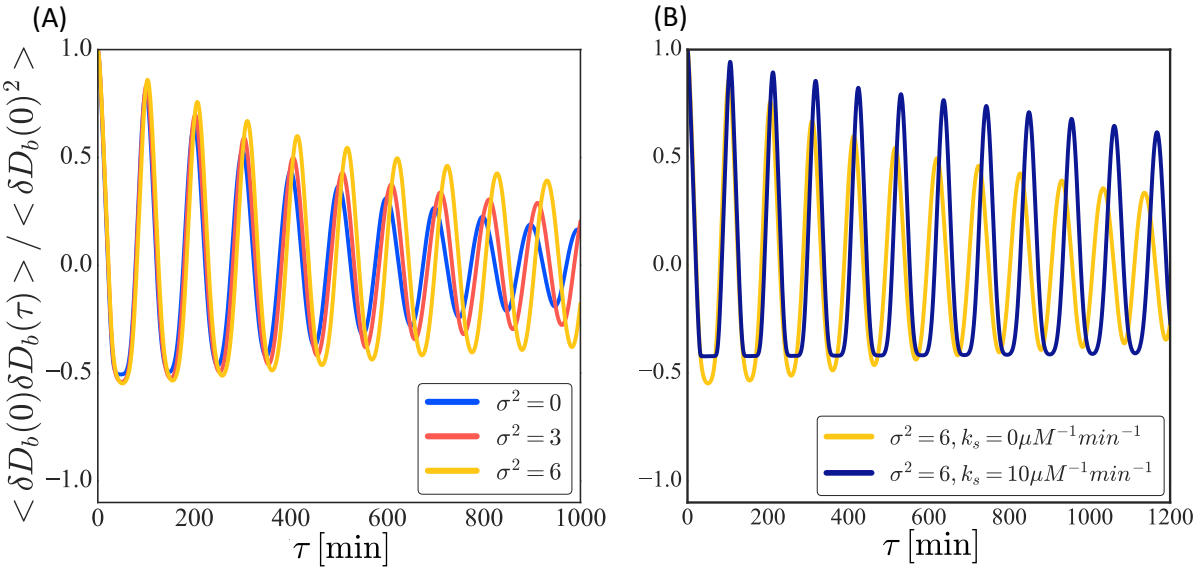


Figure 5: (A) Normalized autocorrelations of steady-state fluctuations ($\alpha = 0.25min^{-1}$) in a $NF\kappa B - DNA(D_b)$ population for Distributed binding sites whose unbinding rates follow a LogNormal Distribution( $< \ln(k_{doff}) >= 0$ and $\sigma^2 = 0, 3, 6$ for $\ln(k_{doff})$). (B) Normalized autocorrelation of steady-state fluctuations ($\alpha = 0.25min^{-1}$) in a $D_b$ population with distributed binding sites ($\sigma^2 = 6$ for $\ln(k_{doff})$) and molecular stripping enabled ($< \ln(k_{doff}) >= 0$).

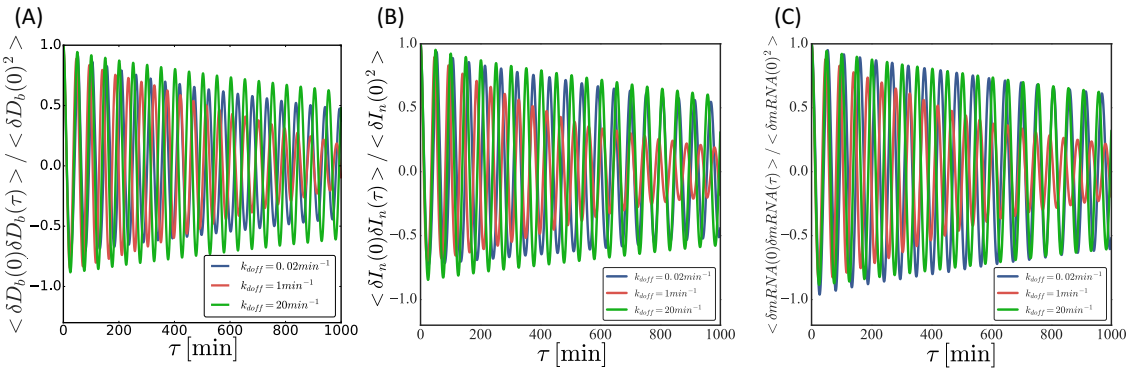


Figure 6: (A) Normalized Autocorrelations of steady-state fluctuations of $NF\kappa B - DNA$ complex ($D_b$) population for identical DNA sites with different unbinding rates ($\alpha = 0.55min^{-1}$). (B) Normalized Autocorrelations of steady-state fluctuations of nuclear $I\kappa B$ ($I_n$) population for identical DNA sites with different unbinding rates ($\alpha = 0.55min^{-1}$). (C)Normalized Autocorrelations of steady-state fluctuations of $mRNA$ population for identical DNA sites with different unbinding rates ($\alpha = 0.55min^{-1}$). .

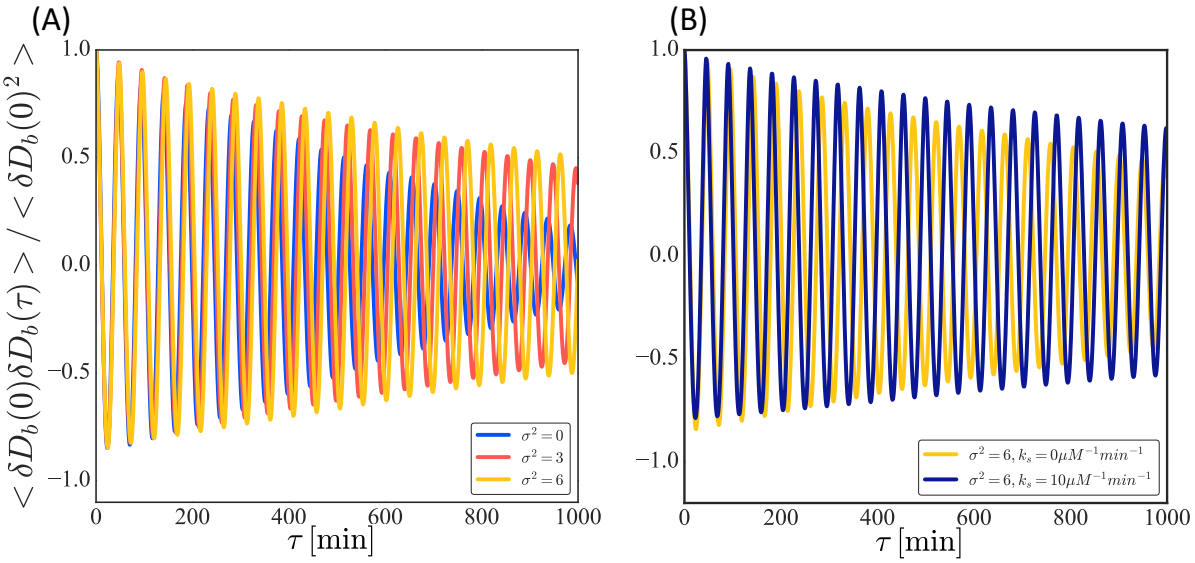


Figure 7: (A) Normalized autocorrelations of steady-state fluctuations ($\alpha = 0.55min^{-1}$) in a $NF\kappa B - DNA(D_b)$ population for Distributed binding sites whose unbinding rates follow a LogNormal Distribution( $< \ln(k_{doff}) >= 0$ and $\sigma^2 = 0, 3, 6$ for $\ln(k_{doff})$). (B) Normalized autocorrelation of steady-state fluctuations ($\alpha = 0.55min^{-1}$) in a $D_b$ population with distributed binding sites ($\sigma^2 = 6$ for $\ln(k_{doff})$) and molecular stripping enabled ($< \ln(k_{doff}) >= 0$).

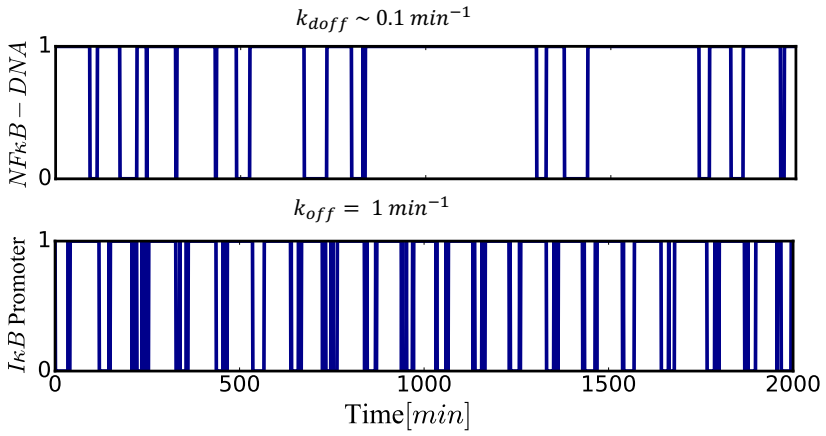


(a)

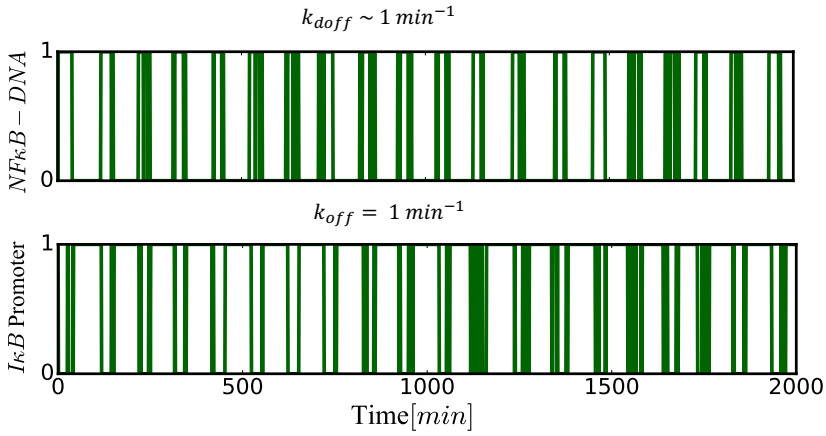


(b)

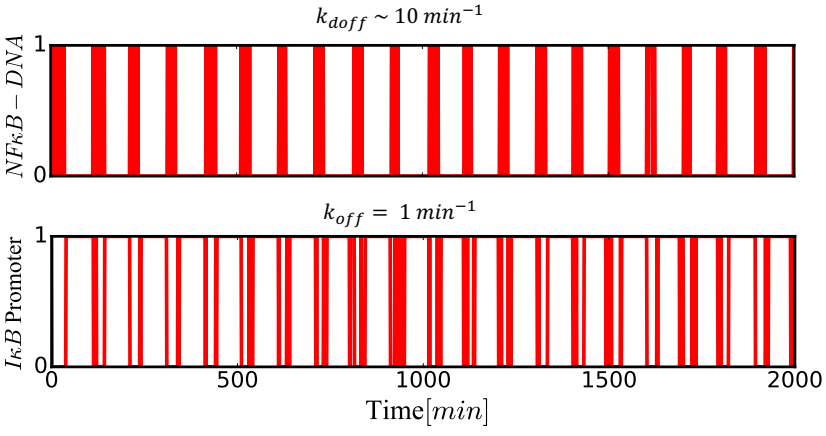


(c)

Figure 8: (a)-(c) Stochastic Trajectories of $NF\kappa B-DNA$ and $I\kappa B$ promoter ($\alpha = 0.25min^{-1}$). (a) Slow Decoy unbinding ($k_{doff} \sim 0.1min^{-1}$). (b) In-resonance Decoy unbinding ($k_{doff} \sim 1min^{-1}$). (c) Fast Decoy unbinding ($k_{doff} \sim 10min^{-1}$).

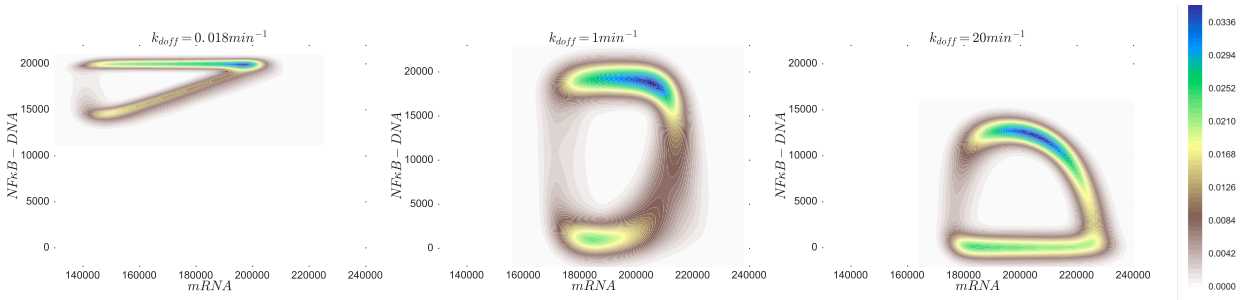


(a)

Figure 9: (a) Stationary probability distribution of noisy limit cycles ($\alpha = 0.55 min^{-1}$) as a function of unbinding rates of decoys in the phase space of $NF\kappa B - DNA(D_b)$ and $mRNA$, no molecular stripping involved.

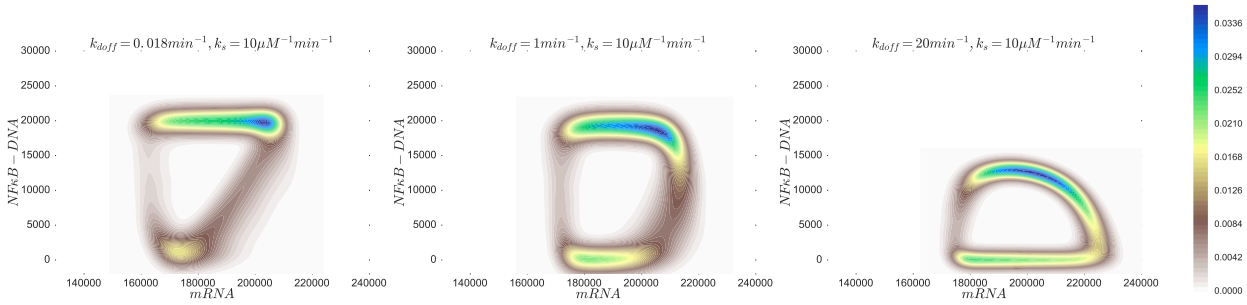


(a)

Figure 10: (a) Stationary probability distribution of noisy limit cycles ($\alpha = 0.55 min^{-1}$) as a function of unbinding rates of decoys in the phase space of $NF\kappa B - DNA(D_b)$ and $mRNA$, molecular stripping rate $k_s = 10 \mu M^{-1} min^{-1}$.

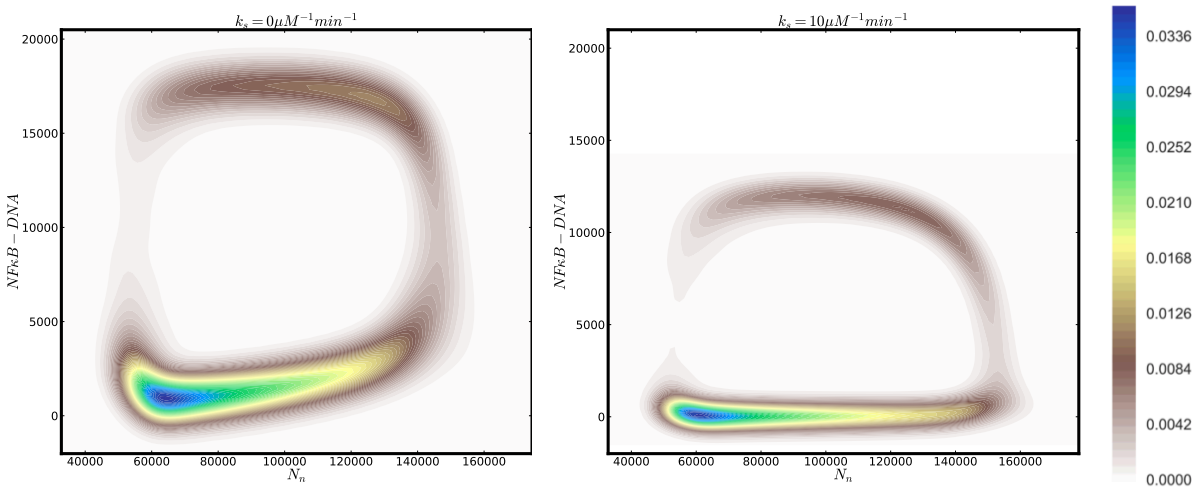


Figure 11: Stationary probability distribution of noisy limit cycles ($\alpha = 0.25min^{-1}$) in the phase space of $N_n$ and $NF\kappa B - DNA$ complex ($D_b$) for distributed decoys whose unbinding rates follow a log-normal distribution, with mean $< \ln k_{doff} >= 0$ and the variance ($\sigma^2$) of $\ln k_{doff}$ be $\sigma^2 = 6$. The left subfigure is the noisy limit cycle without molecular stripping ($k_s = 0\,\mu M^{-1}min^{-1}$); the right subfigure is the noisy limit cycle with molecular stripping ($k_s = 10\,\mu M^{-1}min^{-1}$)

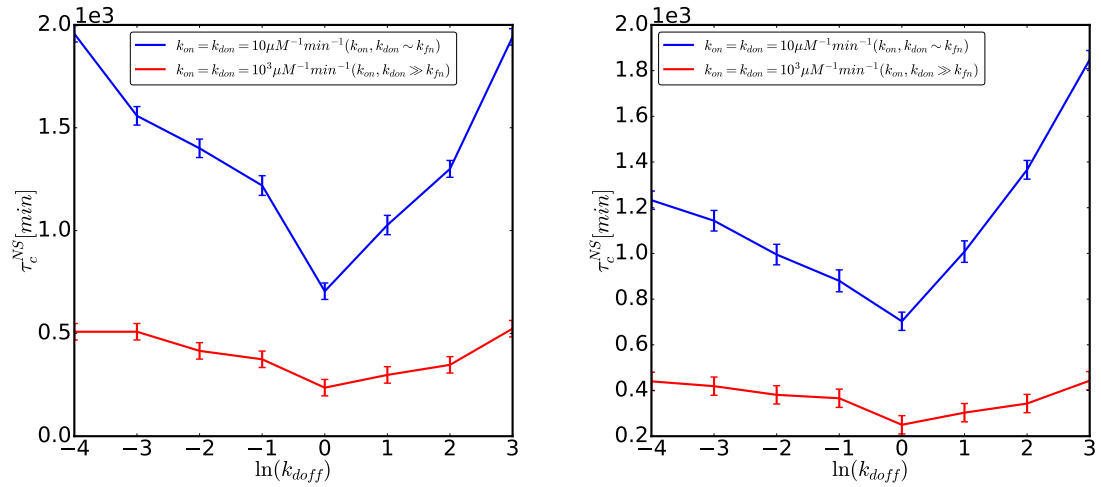


(a) (b)

Figure 12: (a) **Effect of binding rates $k_{don}$ and $k_{on}$ on the stochastic oscillations**: Dephasing time of stochastic $mRNA$ oscillations ($\alpha = 0.55min^{-1}$) as a function of unbinding rates of decoys $\ln(k_{doff})$, no molecular stripping involved. (b) Dephasing time of stochastic $NF\kappa B - DNA$ ($D_b$) oscillations ($\alpha = 0.55min^{-1}$) as a function of unbinding rates of decoys $\ln(k_{doff})$, no molecular stripping involved.

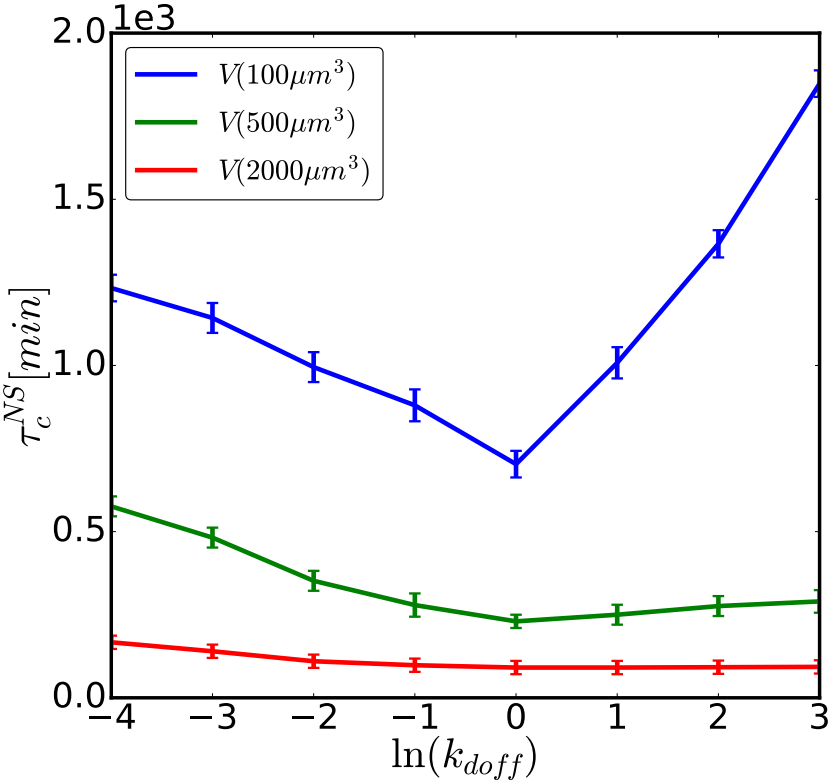


Figure 13: Dephasing Time ($\tau_c^{NS}$) in the absence of molecular stripping as a function of unbinding rates ($k_{doff}$) of Decoys in three different sizes of cell volume (100, 500, 2000 $\mu m^3$.) ($\alpha = 0.55 min^{-1}$)

# References


[1] A. Hoffmann, A. Levchenko, M.L.Scott and D. Baltimore. The I$\kappa$B-NF-$\kappa$B signaling module: temporal control and selective gene activation. *Science*, 298:1241, 2002.

[2] D.W.Scott. On optimal and data-based histograms. *Biometrika*, 66:605, 1979.

[3] S. Bergqvist, V. Alverdi, B. Mengel, A. Hoffmann, G. Ghosh and E. A. Komives. Kinetic enhancement of NF-$\kappa$BDNA dissociation by I$\kappa$B$\alpha$. *Proc. Natl Acad. Sci. USA*, 106:19328, 2009.

[4] T.Siggers et al. Principles of dimer-specific gene regulation revealed by a comprehensive characterization of NF-$\kappa$B family DNA binding. *Nature Immunology.*, 107:4016, 2010.

[5] V. Alverdi, B. Hetrick, S. Joseph, E.A.Komives. Direct observation of a transient ternary complex during I$\kappa$B$\alpha$-mediated dissociation of NF-$\kappa$B from DNA. *Proc. Natl Acad. Sci. USA*, 111:225, 2014.